Investigation of Ionospheric Response to Severe Magnetic Storms Using GPS Total Electron Content Measurements

M. Fedrizzi[1,*] , E. R. de Paula[1], I. J. Kantor[1], R. B. Langley[2], A. Komjathy[3], Eduardo A. Araujo-Pradere[4], Timothy J. Fuller-Rowell[4]

[1]*Divisão de Aeronomia, Instituto Nacional de Pesquisas Espaciais, C.P. 515, São José dos Campos, SP 12245-970, Brazil*

[2]*Department of Geodesy and Geomatics Engineering, University of New Brunswick, Fredericton, NB E3B 5A3, Canada*

[3]*Jet Propulsion Laboratory, California Institute of Technology, M/S 238-634A, 4800 Oak Grove Drive, Pasadena, CA 91109, USA*

[4]*Space Environment Center, NOAA, 325 Broadway, Boulder, CO 80305, USA*

Abstract

Data collected from several Global Positioning System (GPS) networks worldwide have been used along with ionosonde measurements to investigate the ionospheric response to severe magnetic storms, which occurred on July 15, 2000 and on March 31, 2001. For this purpose, the University of New Brunswick Ionospheric Modelling Technique (UNB-IMT), which applies a spatial linear approximation of the vertical TEC above each station using stochastic parameters in a Kalman filter estimation, has been used to describe the local time and geomagnetic latitude dependence of the TEC. Analysis of the results showed an ionospheric response dependent on the local time and magnetic conditions previous to and during the storm period. The two most interesting phenomena observed in the ionosphere over the South-American sector during the July 15, 2000 storm were (i) a significant intensification of the fountain effect due to an eastward magnetospheric electric field penetration into the equatorial ionosphere, causing TEC enhancements larger than 200% on the equatorial anomaly crests, which were displaced towards magnetic latitudes up to ± 30° and (ii) ionization depletions caused by storm induced neutral gas composition changes transported by thermospheric winds flowing from high to low latitudes. During the March 31, 2001 storm, the global ionosphere showed a distinctly different behaviour over the Australian/Asian and American regions, which are located at approximately opposite longitude sectors. The southward turning of the interplanetary magnetic field during the recovery phase of this storm began a process of substorm activity and development and intensification of electrojet activity in high-latitude regions and a renewed build-up of the ring current. During this phase, the equatorial anomaly development appeared to be less effective in the American sector compared to the Australian/Asian sector in the first hours of this initial period of activity. Ionosonde measurements indicate that mechanisms like prompt penetration and disturbance dynamo electric fields and thermospheric winds play an important role in this ionospheric behaviour.

1. Introduction

Monitoring the ionosphere with the Global Positioning System (GPS) is currently a widely used procedure, on both global and regional scales (e.g., Coster et al., 2003; Maruyama et al., 2004b; Tsurutani et al., 2004). Owing to its continuous operation and the large number of worldwide receivers, GPS is a powerful tool to investigate ionospheric structures, mainly during magnetically disturbed periods when dynamics and energy dissipation processes in the magnetosphere-thermosphere-ionosphere system become extremely complex (e.g., Prölss, 1995; Fuller-Rowell et al., 1997).

Computing the total electron content (TEC) from GPS data is feasible due to the dispersive nature of the ionosphere, which affects the speed of propagation of the electromagnetic waves transmitted by the GPS satellites on two L-band frequencies (L1=1575.42 MHz and L2=1227.60 MHz) as they travel through that region of the atmosphere. To first order, the change in satellite-to-receiver signal propagation time due to the ionosphere is directly proportional to the integrated free-electron density along the signal path. GPS pseudorange measurements are increased (the signal is delayed) and the carrier-phase measurements are reduced (the phase is advanced) by the presence of the ionosphere. After forming the linear combination of these measurements on the L1 and L2 frequencies, the carrier phase and the pseudorange TEC are obtained.

In this paper, we discuss the use of GPS data to investigate the response of the ionosphere to the July 15, 2000 and the March 31, 2001 magnetic storms. During the first storm, TEC observations were obtained only for the American sector,

* Now at NOAA-Space Environment Center as an NRC Research Associate (Mariangel.Fedrizzi@noaa.gov).

while for the second storm the global ionosphere is analysed. Besides the Scripps Orbits and Permanent Array Center (SOPAC) data archive networks, we used data from the Brazilian Network for Continuous Monitoring (RBMC), which is an important data source for obtaining more accurate information about the ionosphere in low latitude regions. Ionosonde data from various stations were used to help explain TEC variations observed during those storms. TEC measurements are provided by the University of New Brunswick Ionospheric Modelling Technique (UNB-IMT), which applies a spatial linear approximation of the vertical TEC above each station using stochastic parameters in a Kalman filter estimation, to describe the local time and geomagnetic latitude dependence of the TEC (Komjathy, 1997).

2. UNB Ionospheric Modelling Technique

The UNB Ionospheric Modelling Technique (UNB-IMT) was developed in 1997, in the Department of Geodesy and Geomatics Engineering at University of New Brunswick (UNB), to compute TEC from GPS observables at both L1 and L2 frequencies in order to provide ionospheric corrections to communication, surveillance and navigation systems operating at one frequency. The software estimates the coefficients of a linear spatial approximation of TEC over each station in addition to the satellite and receiver differential biases, modelling the ionospheric measurements from a dual frequency GPS receiver with the single-layer ionospheric model (e.g.,Komjathy, 1997; Komjathy and Langley, 1996).

The single layer ionospheric model assumes that the vertical TEC can be approximated by a thin spherical shell, which is typically located at the height of maximum electron density. In the UNB-IMT approrach, the ionospheric shell height can be a value either fixed or computed by the IRI-95 (International Reference Ionosphere-1995) model (Bilitza, 1997). The combined satellite-receiver differential delays for a reference station are estimated using the Kalman filter algorithm and, in a network solution, additional biases for the other stations in the network are estimated based on the fact that the other receivers have different instrumental delays. Therefore, for each station other than the reference station, an additional differential delay parameter is estimated, which is the difference between the receiver differential delay of a station in the network and the reference station. This technique is described by Sardon et al. (1994). The mapping function we used in our work is the standard geometric mapping function, which computes the secant of the zenith angle of the signal geometric ray path at the ionospheric pierce point at a shell height computed by IRI-95 (Komjathy, 1997).

Due to the dependence of the ionosphere on solar radiation and the geomagnetic field, a solar-geomagnetic reference frame is used to compute the TEC at each station. Since the ionosphere changes more slowly in the Sun-fixed reference frame than in the Earth-fixed one, using such a reference frame results in more accurate ionospheric delay estimates when the Kalman filter is applied (Komjathy, 1997). The ionospheric model was evaluated for the four geographically closest stations to a grid node at which a TEC value is computed. Subsequently, the inverse distance squared weighted average of the individual TEC data values for the four GPS stations were computed.

3. Observations and Discussions

UNB-IMT has been used to examine the spatial end temporal variation of TEC during two intense magnetic storms: the July 15, 200 and the March 31, 2001 storms. In this study, we used data obtained from International GPS Service (IGS), Brazilian Network for Continuous Monitoring (RBMC) and Scripps Orbits and Permanent Array Center (SOPAC) data archive networks. For the July 15 storm investigation, we focused in the South American region, while for the March 31 storm the global ionosphere was analysed. These variations have been interpreted with the help of geomagnetic measurements and ionosonde data.

3.1. July 15 Magnetic Storm

Well known as the “Bastille Day” and “St. Swithin’s Day” storm, the July 15, 2000 magnetic storm is considered one of the most intense storms occurring during the last decade. Figure 1 shows a summary of the solar wind and geomagnetic conditions for the period July 13 to July 17. On July 15, the north-south component (Bz) of the interplanetary magnetic field (IMF) (top panel) exhibited a significant incursion to the south that lasted about 5 hours, reaching the magnetopause with a minimum value of approximately -60 nT at 20:10 UT. In the middle panel, the auroral electrojet (AE) index showed values larger than 1000 nT for at least half a day, reaching values up to 3000 nT. In the bottom panel, the longitudinally symmetric (SYM-H) disturbance index showed a first sudden storm commencement (SSC) at 14:39 UT, followed by a decrease to –74 nT at 16:55 UT; a second SSC occurred at 19:08 UT, and the SYM-H reached –347 nT at 21:54 UT. We have used the SYM-H index instead of the disturbance storm time (Dst) index, since its one-minute resolution is more appropriate for studies of phenomena occurring on a short time scale. The SYM-H index follows essentially the same

variations as the Dst index, however it is obtained from a different set of stations and a slightly different coordinate system (Iyemori et al., 2003). Also, in the bottom panel, the Kp index indicated intense activity during the entire day, reaching values larger than 8 that lasted for about 12 hours. The IMF data were obtained at http://cdaweb.gsfc.nasa.gov/; AE and SYM-H, at http://swdcwww.kugi.kyoto-u.ac.jp/; and Kp, at ftp://ftp.ngdc.noaa.gov/STP/GEOMAGNETIC_DATA/.

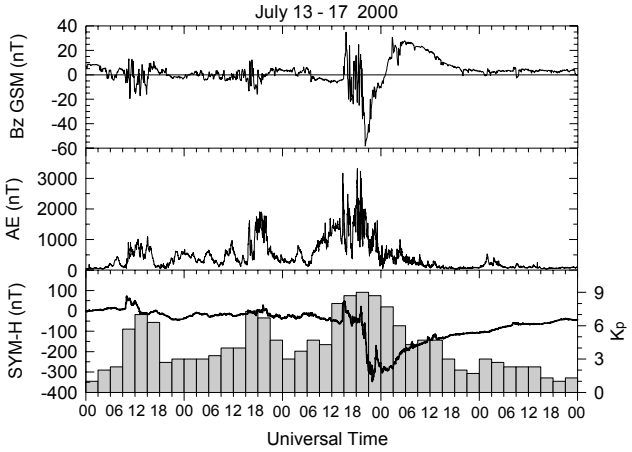

Figure 1. Bz component of the interplanetary magnetic field in geocentric-solar-magnetospheric (GSM) coordinates provided by the Advanced Composition Explorer (ACE) spacecraft for the period July 13-17, 2000 (top); AE index (middle); and SYM-H and Kp indices for the same period (bottom). In the top panel, the time delay of the magnetic field convection from ACE to the magnetopause was taken into account.

The region covered by the TEC maps in our first study is shown by the red box shown in Figure 2. However, we used data from 33 to 37 stations (depending on the day) located between 70°S and 30°N geographic latitude and 150°W and 40°E geographic longitude for data processing, in order to obtain reliable values for the TEC over the oceanic area bordering South America, where there are very few GPS stations. The quality of the GPS data was checked for all stations using the Translate/Edit/Quality Check (TEQC) software (UNAVCO, 2004). Based on the QC results, we have chosen Rio Grande (geographic coordinates: 53.79°S, 67.75°W) as the reference station since, amongst the stations located in a geomagnetic mid-latitude region where the ionosphere is fairly well behaved, it had the best results in terms of data quality during the period analysed (July 13-18, 2000). Also, TEC maps were produced using a 5-degree grid spacing and 1-hour resolution, so that each map contains the observations obtained from 30 minutes before to 30 minutes after the respective hour. The ionosphere shell height value was fixed and set to 400 km.

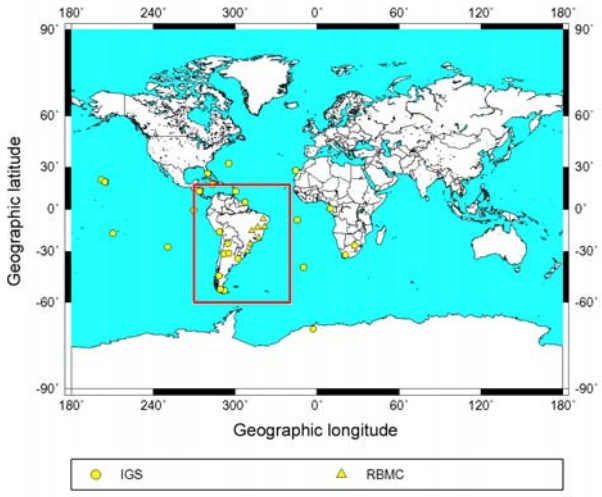

Figure 2. Map showing the International GPS Service and the Brazilian Network for Continuous Monitoring GPS stations used for the July 15, 2000 magnetic storm study. The region analysed is located inside the red box.

TEC maps for this magnetic storm have already been shown by Fedrizzi et al. (2001), therefore in this paper we will concentrate on meridional cross sections along specific longitudes in order to better visualize the TEC depletions and enhancements. The equatorial anomaly development over the longitude 290°E is shown in Figure 3. During this event, TEC increases over the South American region starting at 16:00 UT on July 15, however the equatorial anomaly begun its development around 19:00 UT, reaching its maximum around 22:00-23:00 UT. It is evident that as time advances, TEC increased on both sides of the magnetic equator and the equatorial anomaly crests were displaced toward higher latitudes. This behaviour is most likely associated with the fountain effect intensification due to the penetration of an eastward electric field into the equatorial ionosphere, which forces a large amount of plasma to be uplifted at the magnetic equator and to subsequently diffuse along the magnetic field lines towards higher latitudes. A low latitude digisonde station in Brazil (Cachoeira Paulista, geographic coordinates: 22.7°S, 45.0°W; geomagnetic latitude: 17.6°S) registered a very significant increase of the F2 layer peak height (hmF2) from 400 to 600 km at about 20:00 UT (17:00 LT) on July, 15 (Figure 4), confirming the plasma uplift occurrence. Additionally, a comparison between TEC on the storm and adjacent days (Figure 5) shows the significant plasma depletion over the magnetic equator at 22:00 UT (19:00 LT), along longitude 315°E over the Brazilian region. Using measurements provided by the Defense Meteorological Satellite Program (DMSP) satellites, Basu et al. (2001a) have also shown deep ion density depletions over the same region.

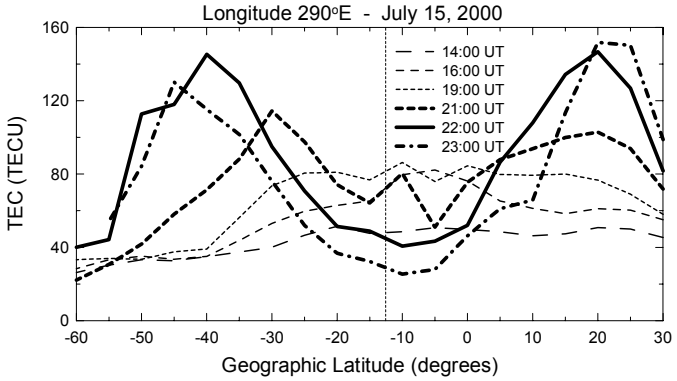

Figure 3. Latitudinal variation of TEC along geographic longitude 290°E, on July 15, showing the equatorial anomaly development on that day. The vertical dotted line indicates the location of the geomagnetic equator.

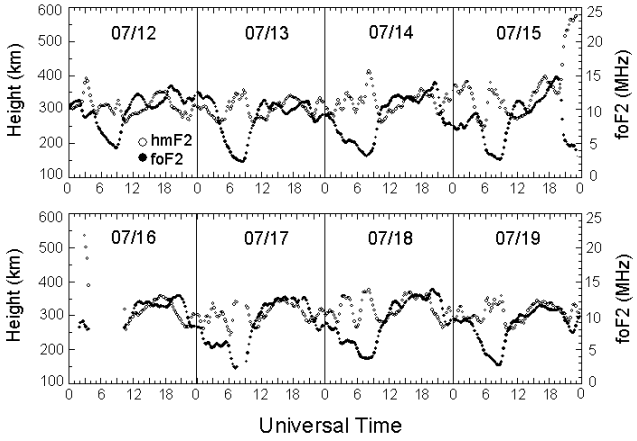

Figure 4. F2 layer peak height (hmF2) and F2 layer critical frequency (foF2) obtained from digisonde measurements at Cachoeira Paulista for the period July 12-19, 2000.

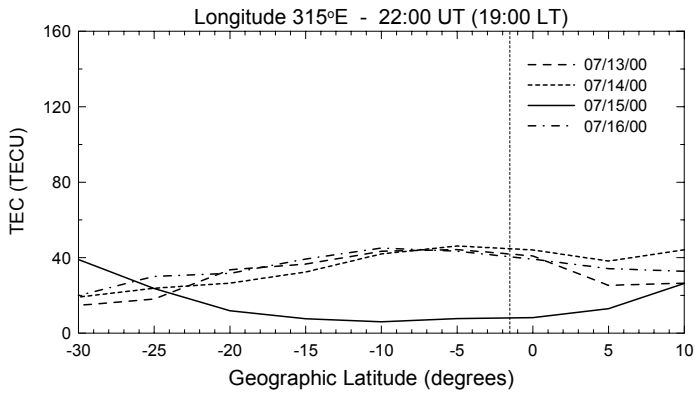

Figure 5. Latitudinal variation of TEC along geographic longitude 315°E for the period July 13-16, 2000, at 22:00UT, showing TEC depletion on July 15. The vertical dotted line indicates the location of the geomagnetic equator.

During this storm, decreases in the ionization density characterizing the negative phase of ionospheric storms were also observed over the north of South America, reaching values up to 70-80% smaller than the TEC observed two days prior to the storm commencement (Figure 6). The negative phase was observed to last more than 24 hours (from about 9 UT on July 16 to 11 UT on July 17). Interactions between seasonal and storm-induced thermospheric winds are the most probable reason for this observed behaviour. In summer, both types of winds are in phase and the composition disturbance zone is transported much further equatorwards, producing negative phases of an ionospheric storm (Prölss et al., 1991; Prölss, 1995; Fuller-Rowell, 1997; Buonsanto, 1999). Figure 6 also includes the output from a second assimilation model MAGIC (Spencer et al., 2004), extending the region of study into North America on July 14 and July 16, which confirms that a negative phase had occurred in that region. MAGIC is a Kalman-filter-based data assimilation algorithm for imaging the Earth's ionosphere in four dimensions using GPS data, being the result of a Space Environment Center (SEC) - National Geodetic Survey collaboration, and is the foundation of the SEC's Real Time U.S.-TEC test product (http://sec.noaa.gov/ustec/) (Araujo-Pradere et al., 2004).

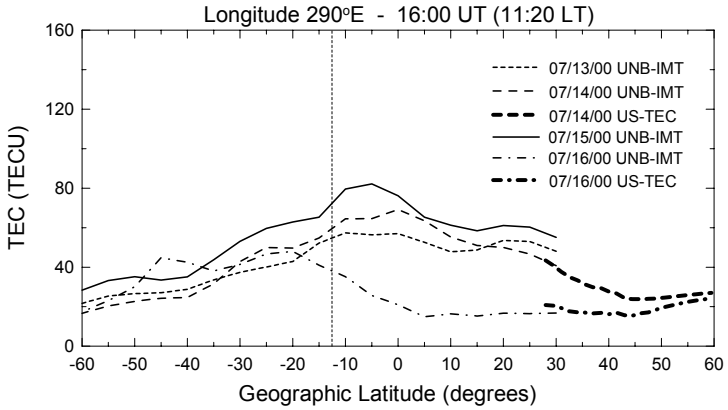

Figure 6. Latitudinal variation of TEC along geographic longitude 290°E, for the period July 13-16, 2000, at 16:00 UT, showing the negative phase on July 16. The vertical dotted line indicates the location of the geomagnetic equator.

3.2. March 31 Magnetic Storm

The intense geomagnetic storm that occurred on March 31, 2001 was particularly interesting because it caused a different ionospheric response in the Australian/Asian sector and the American sector when they were located on dayside. A summary of the solar wind and geomagnetic conditions for the period March 30 to April 3 is presented in Figure 7. On March 31, Bz (top panel) exhibited two significant incursions to the south: the first one lasted about 4 hours and the second one approximately 8 hours. In the middle panel, the AE index shows the significant amount of energy that was injected at high latitudes during the storm period. In the bottom panel, the SYM-H disturbance index showed a first SSC at 00:52 UT, and a second one at 02:51 UT. The third SSC occurred at 04:07 UT, and SYM-H reached –437 nT at 08:07 UT. Also, in the bottom

panel, the Kp index indicated intense activity during the entire day, reaching values of 9^- that lasted for about 6 hours. The IMF, AE, SYM-H and Kp data were obtained from the sources cited in the previous section.

In order to study the TEC response during this storm period, we have processed data from about 250 stations distributed worldwide (Figure 8), and Albert Head station (geographic coordinates: 48.4°N, 123.5°W) was chosen as the reference station. TEC maps were produced using 5-degree grid spacing, however we have increased their time resolution to 15 minutes, so that each map contains the observations obtained from 7.5 minutes before to 7.5 minutes after the respective quarter hour (Fedrizzi et al., 2004). The ionosphere shell height value was obtained from IRI-95 by computing the median height at which the topside and bottomside electron contents are equal. Similar to the previous event, we present TEC along meridional cross sections over specific longitudes, in order to compare its depletions and enhancements.

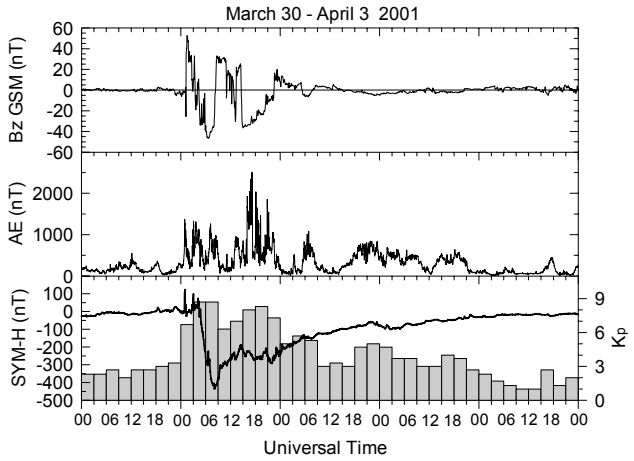

Figure 7. Bz component of the interplanetary magnetic field in geocentric-solar-magnetospheric (GSM) coordinates provided by the Advanced Composition Explorer (ACE) spacecraft for the period March 30-April 3, 2001 (top); AE index (middle); and SYM-H and Kp indices for the same period (bottom). In the top panel, the time delay of the magnetic field convection from ACE to the magnetopause was taken into account.

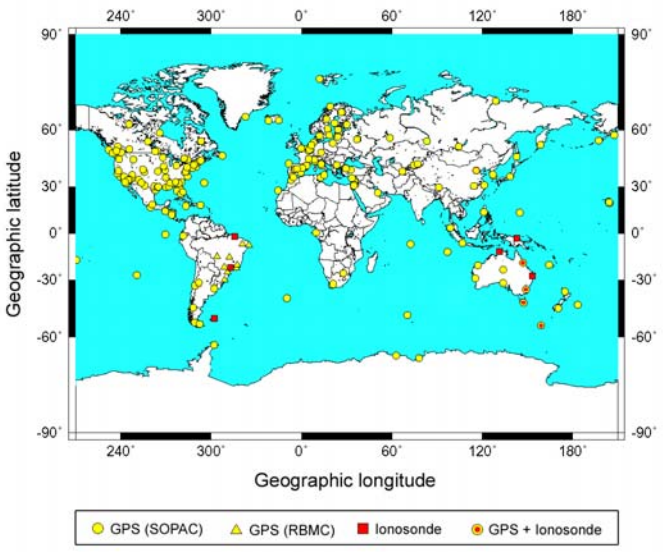

Figure 8. Map showing GPS and ionosonde stations used in the March 31, 2001 magnetic storm study.

The first TEC enhancements on March 31 were observed over the Pacific Ocean, after 01:00 UT. The largest TEC values occurred around 07:00-08:00 UT, over the Australian/Asian sector. An illustration of these enhancements over the longitude 120°E, at 07:15 UT (15:15 LT), is shown in Figure 9. As a comparison, TEC for two quiet days plus the day following the storm are also shown. The error bars give an idea of size of the residuals, which are the differences between the TEC observed at the closest station to the longitude 120°E and the TEC interpolated for that longitude. Plasma depletions were also observed during this period over the magnetic equator. Amongst the possible causes for TEC enhancements over the Australian/Asian sector are (i) the fountain effect intensification due to an eastward magnetospheric electric field penetration into the equatorial ionosphere and (ii) the storm-time thermospheric disturbance winds flowing towards lower latitude regions transporting the ionization upwards along the magnetic field lines to regions where recombination rates are lower. The effectiveness of these winds in modifying the ionospheric height is maximum at middle latitudes and minimum at the geomagnetic equator due to the dip angle. In equatorial latitudes, ionospheric height modifications are mainly associated with electric field influences.

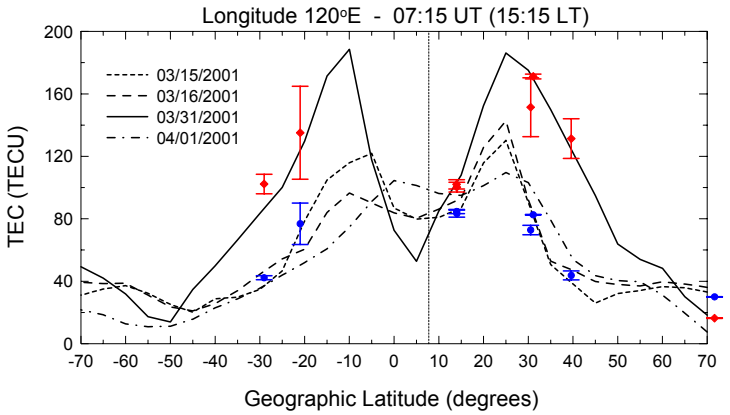

Figure 9. Latitudinal variation of TEC along geographic longitude 120°E, on March 15, 16, 31 and April 1, 2001, at 07:15 UT. The error bars show the residuals, which are the difference between the TEC observed at the closest stations to the longitude 120°E (diamond: March 31; circle: March 15) and the TEC interpolated for that longitude. The vertical dotted line indicates the location of the geomagnetic equator.

Measurements of the F-region minimum virtual height (h'F) and the height of peak electron density (hmF2) obtained from seven ionosonde stations located in the Australian region (see Figure 8) showed an uplift of the F2 layer over all stations (Figure 10) presumably due to some combination of eastward electric fields, equatorward storm-time thermospheric winds, and thermal expansion caused by the transport of Joule and particle heating from high latitudes. The ionosonde station closest to the geomagnetic equator (Vanimo, geographic coordinates: 2.7°S, 141.3°E;) registered an uplift of the F2 layer from approximately 04:00 UT (13:25 LT) to 08:00 UT (17:25 LT), which is most likely caused by a magnetospheric eastward electric field penetration into the equatorial ionosphere. The other ionosonde stations in Figure 10 have also shown hmF2 uplifts during that period. The uplifts at these mid latitude stations may be caused by a superposition of electric fields and thermospheric winds/expansion effects, but the relative contribution of each mechanism in raising the F2 layer is uncertain. At high latitudes, equatorward storm-time thermospheric winds and thermal expansion is most likely the dominant mechanisms that uplift the ionosphere.

Around 08:00 UT (17:25 LT), Vanimo registered a decrease in h'F, followed by an uplift of h'F and hmF2 at approximately 12:00 UT (21:25 LT), which lasted more than 6 hours. At this time, a significant amount of energy was already injected at high latitudes and therefore disturbance dynamo electric fields are possibly playing a role during this period. The storm heating at high latitudes drives winds, which due to dynamo action tend to reduce the daytime/evening eastward electric field characteristic of quiet periods (Blanc and Richmond, 1980; Scherliess and Fejer, 1997), weakening the upward plasma drift at the magnetic equator and inhibiting the equatorial anomaly development. Consequently, more plasma is retained at equatorial latitudes and less plasma is transported away from the magnetic equator. This equatorial anomaly inhibition was observed over the Australian/Asian sector (longitude 120°E) at 12:15 UT (20:15 LT) on the storm day (March 31), and it is illustrated in Figure 11. During nighttime/early morning hours, on the other hand, the disturbance dynamo electric field is eastward, uplifting the plasma at the equator. This feature was also registered by the Vanimo ionosonde on March 31, according to Figure10. In the South American sector, disturbance dynamo signatures were also observed over São

Luís station (geographic coordinates: 2.5°S, 44.2°W; see Figure 8) from approximately 07:30 UT to 10:30 UT (04:30 to 07:30 LT) on March 31, according to Figure 12. A peak in both h'F and hmF2 occurred around 08:30 UT (05:30 LT) coinciding with the Bz inversion to north. According to Kelley et al. (1979), sudden IMF northward turnings from a steady southward direction causes a temporary imbalance between the convection related charge density and the charge in the inner edge of ring current, producing a dusk-to-dawn electric field perturbation that can penetrate into the equatorial ionosphere. This magnetospheric electric field is westward during the day and eastward at night. Therefore, it is possible that a superposition of both magnetospheric and disturbance dynamo electric fields has occurred during that time.

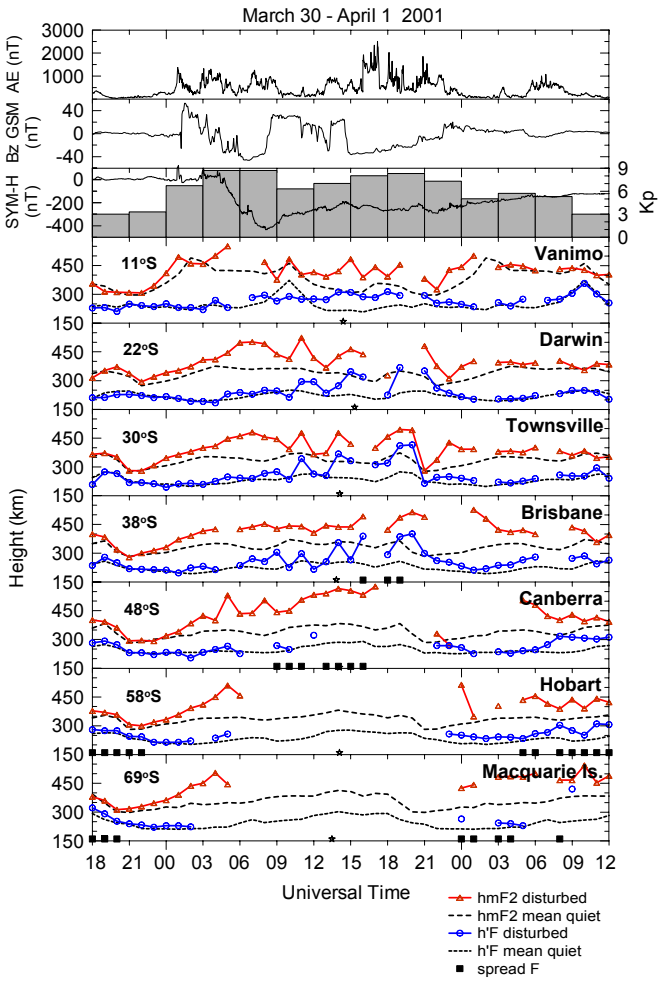

Figure 10. F layer minimum virtual height (h'F) and F2 peak height (hmF2) at ionosondes operated by IPS Radio and Space Services ionosonde network, for the period March 30 to April 1. Bz, AE, SYM-H and Kp values for the same period are shown in the top panels. Midnight local time is indicated by the "star" symbol and the magnetic latitude of each station is provided. The occurrence of spread F is noted.

On March 31, around 08:30 UT, Bz turned northward and remained north until approximately 14:30 UT, then it turned again southward for about 8 hours, beginning a process of substorm activity and development and intensification of electrojet activity over broad regions. During this period, the largest TEC increases over the globe were observed in the American sector, between 19:00 and 20:00 UT. Figure 13 illustrates the TEC enhancements which occurred along the longitude 290°E at 19:30 UT (14:50 LT). For comparison, TEC values observed during two quiet days plus the day following the storm are also shown. At this time, plasma depletions were observed over the magnetic equator, but they were not so conspicuous as the ones observed in the Australia/Asian sector a few hours earlier. During this period, a negative phase of the ionospheric storm was also observed in the north hemisphere, possibly due to a combination of the trough displacement towards lower latitudes and the transport of the composition disturbance zone equatorwards (Prölss et al., 1991; Foster et al.,

2002). According to Field and Rishbeth (1997), in general the behaviour of the ionosphere at equinox during magnetically disturbed periods more closely resembles summer behaviour, rather than winter behaviour.

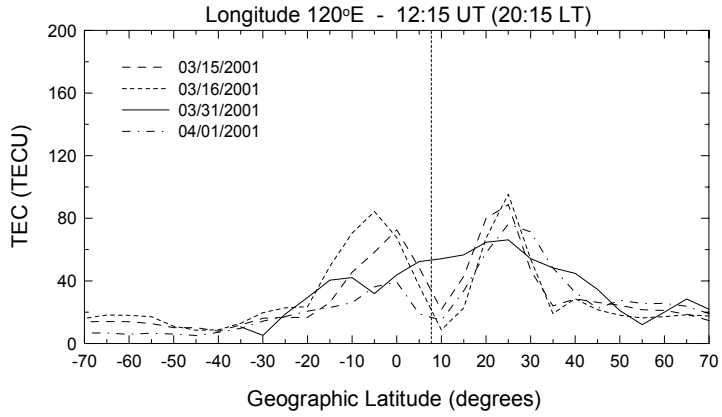

Figure 11. Latitudinal variation of TEC along geographic longitude 120°E, on March 15, 16, 31 and April 1, 2001, at 12:15 UT, showing the equatorial anomaly inhibition on March 31. The vertical dotted line indicates the location of the geomagnetic equator.

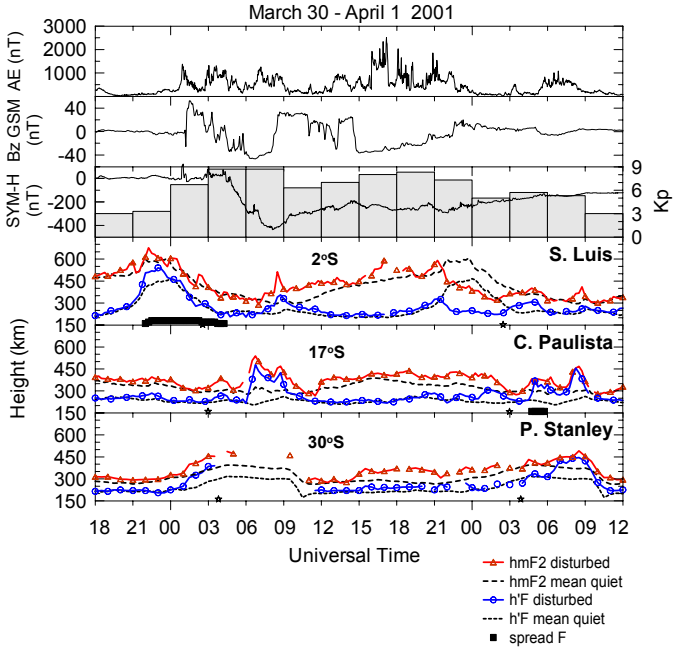

Figure 12. F layer minimum virtual height (h'F) and F2 peak height (hmF2) at ionosondes operated by INPE (São Luís and Cachoeira Paulista) and Rutherford Appleton Laboratory (Port Stanley, whose data were provided by NGDC), for the period March 30-April 3, 2001. Bz, AE, SYM-H and Kp values for the same period are shown in the top panels. Midnight local time is indicated by the "star" symbol and magnetic latitude of each station is provided. The occurrence of spread F is also noted.

Besides São Luís station, Figure 12 shows data obtained from two other ionosonde stations in South America (see Figure 8), Cachoeira Paulista (geographic coordinates: 22.7°S, 45.0°W) and Port Stanley (geographic coordinates: 51.6 °S, 57.9°W), which are used to help identify possible causes for the TEC enhancements. On March 31, hmF2 above the São Luís station showed an uplift between 15:00 UT (12:00 LT) and 19:00 UT (16:00 LT), which may be associated with a plasma uplift due to the penetration of an eastward magnetospheric electric field into the equatorial ionosphere. During the same period, ionosonde stations located further south showed hmF2 uplifts, which are probably due to the presence of disturbed

thermospheric winds flowing equatorwards. The hmF2 uplift was not so conspicuous in the South American sector, possibly due to the geomagnetic pole offset from the geographic ones. A few hours later, h'F and hmF2 showed a decrease from about 22:00 to 03:00 UT (19:00 to 24:00 LT), followed by an uplift lasting until 06:00 UT (03:00 LT) on April 1. The inhibition of the post-sunset uplift of the F layer over São Luís (equatorial station located at longitude 315.8°E) is in agreement with TEC observations presented in Figure 14, which is typical of the disturbance dynamo electric field action.

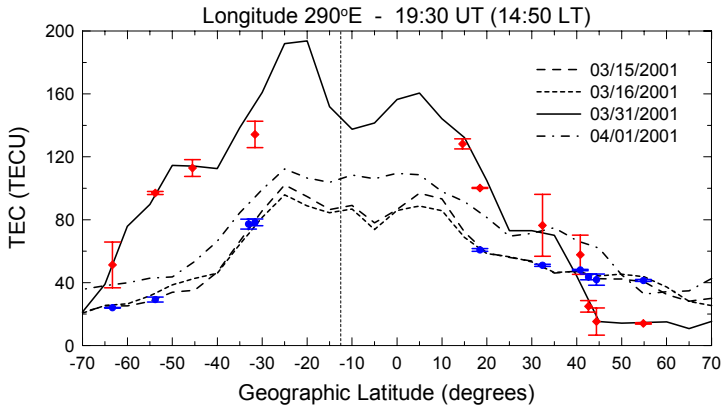

Figure 13. Latitudinal variation of TEC along geographic longitude 290°E, on on March 15, 16, 31 and April 1, 2001, at 19:30 UT. The error bars show the residuals, as in Figure 9. The vertical dotted line indicates the location of the geomagnetic equator.

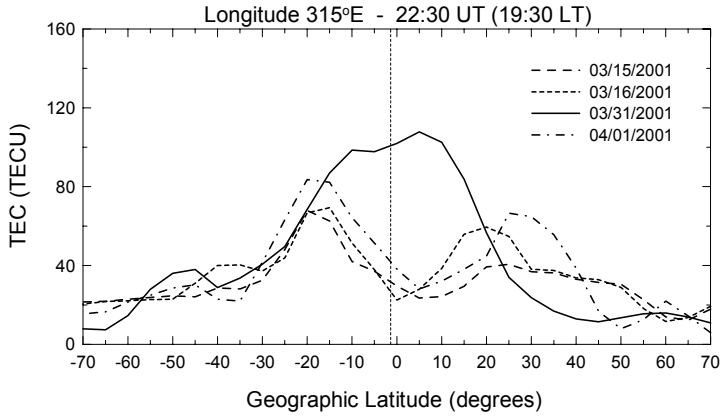

Figure 14. Latitudinal variation of TEC along geographic longitude 315°E, on March 15, 16, 31 and April 1, 2001, at 22:30 UT, showing the equatorial anomaly inhibition on 03/31. The vertical dotted line indicates the location of the geomagnetic equator.

It is worth noting that the TEC response over the Brazilian sector during the July 15, 2000 and March 31, 2001 magnetic storms were quite different. When comparing Figures 5 and 14, even though there is only a 30-minute time difference between them, it seems clear that the mechanisms playing a role during that time are either different or possibly a combination of various elements. During the first storm, TEC was depleted at the magnetic equator mainly due to a magnetospheric eastward electric field penetration while in the second case, plasma was retained in that region primarily due to a westward disturbance dynamo electric field. During the July 15 storm, the main energy input occurred when it was daytime in the American sector and nightime in the Australian/Asian sector. On the other hand, the March 31 storm main energy input began when it was daytime in the Australian/Asian sector and nightime in the American sector. Also, the storm development and recovery lasted longer for the March 31 storm than it did for the July 15 storm. Therefore, not only the ionospheric response to magnetic storms depends strongly on local the time at the storm commencement, but also on the storm development and recovery duration, agreeing with reports in the literature (e.g., Prölss, 1995, and references therein; Basu et al., 2001b). Thanks to the large number of worldwide GPS receivers in continuous operation, it is currently possible to obtain a global picture of the ionosphere and its structures. These data can significantly contribute to the understanding of

the dynamics and energy dissipation processes in the magnetosphere-thermosphere-ionosphere system during magnetically disturbed periods.

4. Summary and Future Considerations

We have used GPS data to investigate the responses of the ionosphere to the July 15, 2000 and the March 31, 2001 magnetic storms using TEC measurements computed using the UNB-IMT data assimilation model. This technique is currently being improved through the investigation of different approaches for modelling the ionosphere with sparse networks and experimenting with different algorithms, such as the quadratic interpolation technique (Rho et al., 2004). Ionosonde data for a few stations located in the South American and Australian regions were also used to help elucidate the possible mechanisms responsible for TEC enhancements and depletions. We have found evidences of magnetospheric and disturbance dynamo electric fields, equatorward storm-time thermospheric winds, and thermal expansion caused by the transport of Joule and particle heating from high latitudes effects. When analysing differences and similarities of TEC response to those storms, we observed a strong dependence on local time at the storm commencement, as well as on storm development and recovery duration. We are currently comparing these results with physical models (Maruyama et al., 2004a) to investigate the importance of each mechanism during the various phases of the storm occurrence.

Acknowledgements

We thank the following institutes for providing data: Scripps Orbit and Permanent Array Center (SOPAC), Brazilian Institute of Geography and Statistics (IBGE), National Institute for Space Research (INPE), IPS Radio and Space Services, National Geophysical Data Center (NGDC) at NOAA, Coordinated Data Analysis Web at NASA/GSFC and the World Data Center for Geomagnetism. E. R. de Paula thanks to CNPq for partial support under Process 502223/91-0. This research was supported by CAPES Foundation (Brazil) and performed while the author was enrolled in a Ph.D. programme at INPE.

References

Araujo-Pradere, E. A., Fuller-Rowell, T. J., Spencer, P. S. J. TEC repeatable changes during ionospheric storms, J. Geophys. Res., 2004 (submitted).

Basu, Su; Basu, S; Groves, K. M.; Yeh, H.-C.; Su, S.-Y.; Rich, F. J.; Sultan, P.J.; Keskinen, M. J. Response of the equatorial ionosphere in the South Atlantic region to the great magnetic storm of July 15, 2000. Geophys. Res. Lett., 28 (18), 3577-3580, 2001a.

Basu, Su, Basu, S, Valladares, C. E., Yeh, H.-C., Su, S.-Y., MacKenzie, E., Sultan, P.J., Aarons, J., Rich, F. J., Doherty, P., Groves, K. M., Bullet, T. W. Ionospheric effects of major magnetic storms during the International Space Weather period of September and October 1999: GPS observations, VHF/UHF scintillations, and in situ density structures at middle and equatorial latitudes. J. Geophys. Res., 106 (A12), 30389-30413, 2001b.

Bilitza, D. International reference ionosphere - Status 1995/96. Adv. Space Res., 20 (9), 1751-1754, 1997.

Blanc, M, Richmond, A. D. The ionospheric disturbance dynamo. J. Geophys. Res., 85 (A4), 1669-1686, 1980.

Buonsanto, M. J. Ionospheric storms: a review. Space Sci. Rev., 88, 563-601, 1999.

Coster, A, Foster, J., Erickson, P., Sandel, B. Monitoring space weather with GPS mapping techniques. Institute of Navigation, Proceedings of the National Technical Meeting 2003, pp. 800-808, Anaheim, CA, January 26-28, 2003.

Fedrizzi, M.; Langley, R. B.; Komjathy, A.; Santos, M. C.; de Paula, E. R.; Kantor, I. J. The Low-Latitude Ionosphere: Monitoring its Behaviour with GPS. Institute of Navigation, Proceedings of ION GPS -2001 pp. 2468-2475, Salt Lake City, September11-14, 2001.

Fedrizzi, M.; de Paula, E. R.; Kantor, I. J., Batista, I. S., Langley, R. B.; Komjathy, A. Study of magnetic storm effects on the ionosphere using GPS data. Adv. Space Res., 2004 (submitted).

Field, P. R.; Rishbeth, H. The response of ionospheric F2-layer to geomagnetic activity: an analysis of worldwide data. J. Atmos. Sol. Terr. Phys., 59 (2), 163-180, 1997.

Foster, J. C.; Erickson, P. J.; Coster, A. J.; Goldstein, J.; Rich, F. J. Ionospheric signatures of plasmaspheric tails. Geophys. Res. Lett., 29 (13), 10.1029/2002GL015067, 2002.

Fuller-Rowell, T. J., Codrescu, M. V., Roble, R. G., Richmond, A. D. How does the thermosphere and ionosphere react to a geomagnetic storm?, in: Tsurutani, B. T., Gonzalez, W. D., Kamide, Y., Arballo, J. L. (Eds.), Magnetic Storms. Washington: American Geophysical Union, 203-225, 1997.

Iyemori, T., Araki, T., Kamei, T., Takeda, M. Mid-latitude Geomagnetic Indices "ASY" and "SYM" for 1999 (Provisional). http://swdcwww.kugi.kyoto-u.ac.jp/aeasy/asy.pdf. Accessed 16 November 2003.

Kelley, M. C., Fejer, B. G. Gonzales, C. A. Explanation for anomalous ionospheric electric fields associated with a northward turning of the interplanetary magnetic field. Geophys. Res. Lett., 6, 301-304, 1979.

Komjathy A., Langley R. B. An Assessment of Predicted and Measured Ionospheric Total Electron Content Using a Regional GPS Network. The Proceedings of the National Technical Meeting of the Institute of Navigation, pp. 615-624, Santa Monica, CA, 22-24 January 1996.

Komjathy, A. Global Ionospheric Total Electron Content Mapping Using the Global Positioning System. 248 pp. (Dept. of Geodesy and Geomatics Engineering, Technical Report No. 188). Ph. D. dissertation. University of New Brunswick, 1997.

Maruyama, N., Fuller-Rowell, T. J., Codrescu, M., Richmond, A. D., Millward, G., Spiro, R. W., Sazykin, S., Toffoletto, F., Lin, C. Relative Importance of Direct Penetration and Disturbance Dynamo Electric Fields on the Storm-Time Equatorial Ionosphere and Thermosphere. Eos Trans. AGU, 85 (17), Jt. Assem. Suppl., Abstract SA42A-06, 2004a.

Maruyama, T., Ma, G., Nakamura, M. Signature of TEC storm on 6 November 2001 derived from dense GPS receiver network and ionosonde chain over Japan. J. Geophys. Res., 109, A10302, doi:10.1029/2004JA010451, 2004b.

Prölss, G. W.; Brace, L. H.; Mayr, H. G.; Carignan, G. R.; Killeen, T. L.; Klobuchar, J. A. Ionospheric storm effects at subauroral latitudes: a case study. J. Geophys. Res., 96 (A2), 1275-1288, 1991.

Prölss, G. W. Ionospheric F-region storms, in: Volland, H. (Ed.), Handbook of Atmospheric Electrodynamics. Boca Raton, FL, CRC Press, 2, 195-248, 1995.

Rho, H., Langley, R. B., Komjathy, A. An enhanced UNB Ionospheric Modeling Technique for SBAS: the quadratic approach. Proceedings of ION GNSS 2004, pp.354-365, Long Beach, CA, September. 21-24, 2004.

Sardón, E., Rius, A., Zarraoa, N. Estimation of the transmitter and receiver differential biases and the ionospheric total electron content from Global Positioning System observations. Radio Sci., 29, 577-586, 1994.

Scherliess, L., Fejer, B. G. Storm time dependence of equatorial disturbance dynamo zonal electric fields. J. Geophys. Res., 102 (A11), 24037-24046, 1997.

Spencer, P. S. J., Robertson, D. S., Mader, G. L. Ionospheric data assimilation methods for geodetic applications. Proceedings of IEEE PLANS 2004, pp. 510-517, Monterey, California, April 26-29, 2004.

Tsurutani, B., Mannucci, A., Iijima, B., Abdu, M. A., Sobral, J. H. A., Gonzalez, W., Guarnieri, F., Tsuda, T., Saito, A., Yumoto, K., Fejer, B., Fuller-Rowell, T. J., Kozyra, J., Foster, J. C., Coster, A., Vasyliunas, V. M. Global dayside ionospheric uplift and enhancement associated with interplanetary electric fields. J. Geophys. Res., 109, A08302, doi: 10.1029/2003JA010342, 2004.

University NAVSTAR Consortium (UNAVCO). TEQC: The Toolkit for GPS/GLONASS Data. http://www.unavco.org/facility/software/teqc/teqc.html. Accessed 14 February 2004.